

Microstructural Evolution in Terms of Porosity in High-Tc Superconductors

Ahmed Ouari, Mohamed Guerioune, Amar Boudour and Youcef Boumaïza

LEREC Laboratory, Department of Physics, Faculty of Sciences, University Badji Mokhtar Annaba,
BP. 12, Annaba 23000, Algérie

Abstract: The low critical current densities of high-Tc superconductors materials can be related to the microstructural imperfections such as pores and microcracks which reduce the effective current carrying cross section. The present study examines the characterisation of the state of microstructure and its evolution during thermal treatment of $\text{YBa}_2\text{Cu}_3\text{O}_{7.8}$. The dilatometric analysis was used to study the shrinkage mechanism during sintering. The microstructure of the sintered samples was characterised in terms of pores distribution and apparent density. Open porosity was measured by mercury porosimeter. In order to compare the results, ultrasonic characterisation such as the longitudinal and transverse wave velocities in the ceramic was carried out. From an ultrasonic point of view, these microstructural features act as inhomogeneities, then the measured ultrasonic parameters will depend on the geometrical arrangement of the microstructure (pores have an effect both on Young's modulus and attenuation).

Key words: Superconductors, porosity, acoustic signature $V(z)$, velocities, elastic parameters

INTRODUCTION

The most important characteristics of a ceramic microstructure are established through densification, microcracks and porosity during sintering. For this, many measurements of the ultrasonic properties both at kHz and MHz frequencies have been made in high Tc superconductors materials^[1-4]. Ultrasonic measurements of elastic constant as a source of information, offer the advantage of being sensitive to densification and micro cracks which influence the fundamental properties of the materials. In other terms, the elastic properties are sensitive to densification and melting (variation of Young's modulus E and shear modulus G). The subsequent increase and decrease in E and G corresponds to elimination of porosity and reflects the varied ratios of the liquid phase. Velocities of ultrasonic waves are related, also, to the elastic properties of the material. So, predictions of longitudinal, transverse and Rayleigh wave velocities (called hereafter V_L , V_T and V_R), are essential in ceramics.

In the present study, first the influence of sintering conditions on densification and porosity of high Tc ceramic superconductors $\text{YBa}_2\text{Cu}_3\text{O}_{7.8}$ (called hereafter Y123), using dilatometry and mercury porosimetry (Poresizer 9310, micromeritics) is reported. In a second stage, theoretical approach using densities of the coupling liquids (water, methanol and mercury) and ultrasonic measurements of V_L and V_T are considered.

According to the theoretical approach for porosity developed, here, the acoustic signature $V(z)$ at the frequency of 30 MHz for the earlier coupling liquids^[5,6] has determined. The treatment of $V(z)$ by FFT^[7] allows to access to VR , E and G ^[8].

RESULTS AND DISCUSSION

The samples were prepared from attrition milled powders. The powder is calcined in air at 850°C for 20 h^[9] and is uniaxially cold pressed at $2t/\text{cm}^2$ to form bars up to 5-6 mm length.

Dilatometric analysis was made in air in order to study the shrinkage mechanism during sintering. Dilatometric curves as a function of temperature are shown in Fig. 1. It indicates that the shrinkage starts at 600°C and increases as the temperature increases. Over 870°C , the samples were found deformed. The maximum shrinkage obtained here is 21 % which corresponds to a final relative density of 84 %. The fracture surface of sintered samples, observed in SEM, shows an important porosity in the temperature range 750°C - 800°C and the grains start to grow at 800°C - 850°C , where as, the porosity is not reduced. At 850°C - 870°C strong grains are formed and become, more and more, faceted. The anisotropy of the form of grains as plate-like started to develop. The complete densification is far from achieved, what with a sintering temperature near the melting point of the materials. From the microstructural point of view,

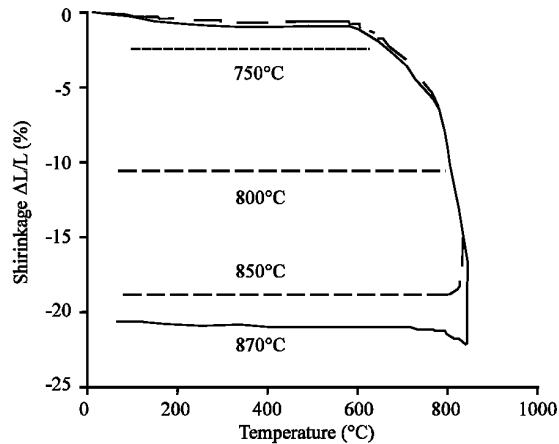
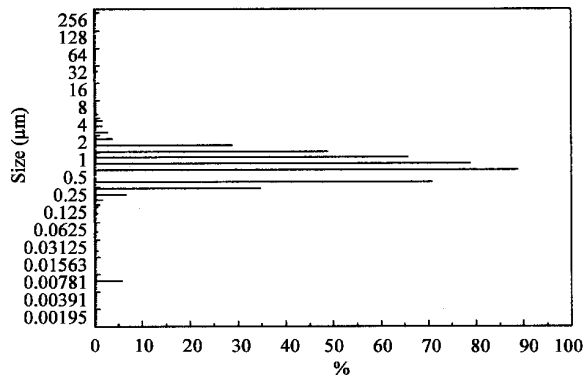
Fig. 1: Dilatometry of Y123 (1h, 2t cm⁻²)

Fig. 2a: Incremental pore volume vs. Pore diameter (at 750°C-800 °C)

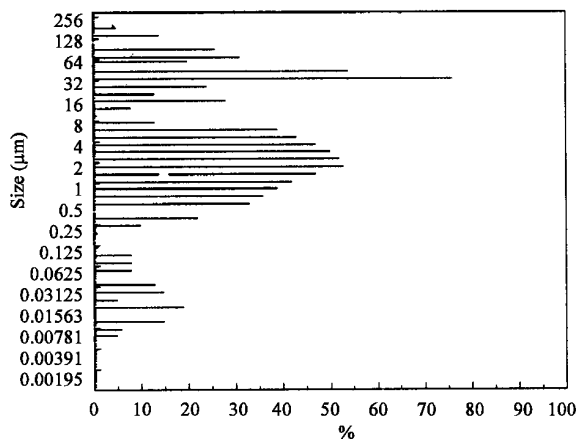


Fig. 2b: Incremental pore volume vs. Pore diameter (at 800°C - 850 °C)

the particle size increases as the sintering temperature increases. The relative density doesn't increase and remains constant at 870°C. There is structural evidence

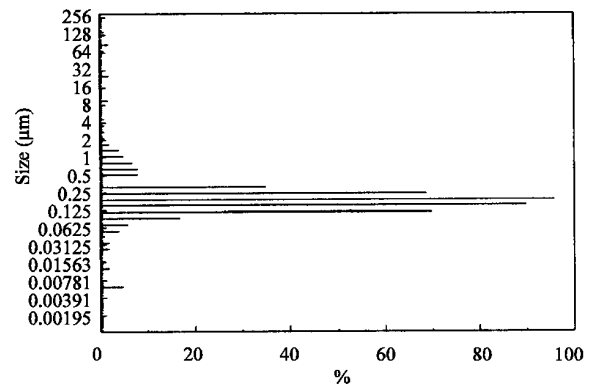


Fig. 2c: Incremental pore volume vs. Pore diameter (at 870°C)

indicating that the Y123 phase is made of plate-like grains randomly oriented and distributed. Observations in SEM and density measurements confirmed the microstructural evolution at 750, 800, 850 and 870°C. The samples sintered in air with 84 % of theoretical density exhibit an average grain size of 13 μm.

Additionally, the microstructure of sintered samples was, also, characterised in terms of pores distribution Fig. 2. In the ranges of temperature 750°C-800°C and 800°C-850°C, the pore distribution is centred at 0.2 μm and 0.5 μm, respectively. At 870°C, samples exhibit two populations of pores in the distribution: one is centred at 1.72 μm and another at 32 μm. So, the large pore distribution is attributed to the microcracks and the creation of open and close porosity which is amplified by the anisotropic growth of plate-like grains randomly distributed.

As the elastic constants and the equivalent wave velocities are closely related to the properties of the Y123 material, an ultrasonic technique is, also, exploited to evaluate the microstructural state. Then, it is interesting to study the influence of the coupling liquids (water, methanol and mercury) on the evolution of $V(z)$ and reflector power $R(\Theta)$ at 30 MHz^[10]. Assuming that these parameters are independent of the grain size for porous material, $V(z)$ and $R(\Theta)$ change as the porosity is eliminated.

Based on the theoretical values V_L and V_T ^[11-13], a program was used to simulate $V(z)$ and $R(\Theta)$ curves. From these curves the different parameters V_R , E and G ^[14] are extracted obtained Table 2. One can see clearly the effect of porosity on the above mentioned parameters.

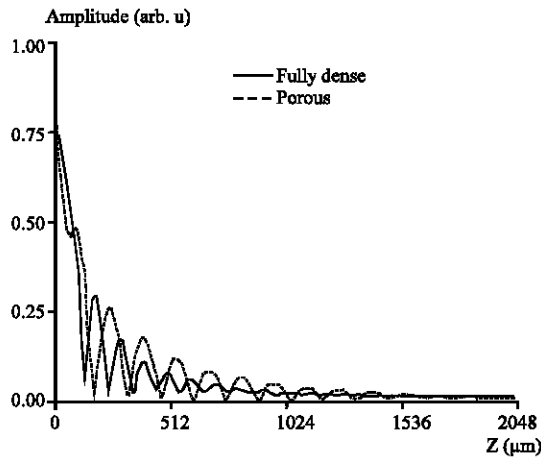
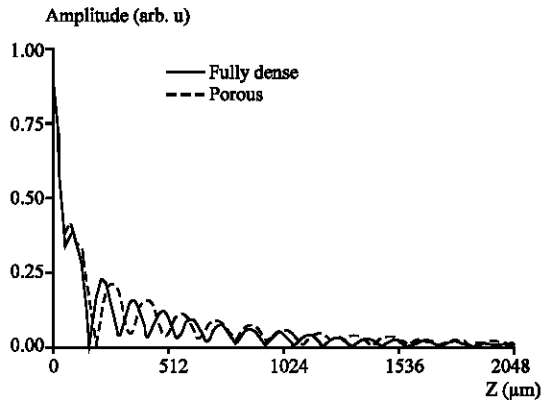
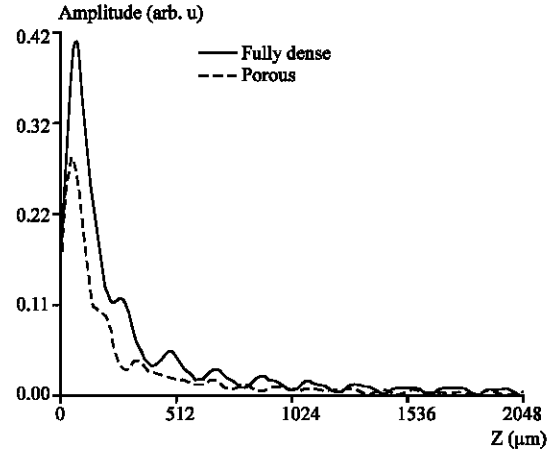
The theoretical $V(z)$ curves Fig. 3a-d show the evolution as a function of different coupling liquids for dense and porous material (20% of porosity). With water as a coupling liquid, the $V(z)$ attenuation exhibits a

Table 1: Variation of density with sintering temperature

T (°C)	750	800	850	870
Dexp/Dth (%)	70	76	80	84
Average pore diameter (μm)	09.65	08.96	04.67	02.38

Table 2: Values of elastic parameters V_R , E and G corresponding to different coupling liquids

Coupling liquid	VR (m/s)	
	Dense	Porous
Water ($V_L = 1497 \text{ m s}^{-1}$)	2620.12	2312.49
Methanol ($V_L = 1103 \text{ m s}^{-1}$)	2664.82	2306.05
Mercury ($V_L = 1450 \text{ m s}^{-1}$)	2666.62	2309.05
Coupling liquid	E (Gpa)	
	Dense	Porous
Water ($V_L = 1497 \text{ m s}^{-1}$)	119.18	77.42
Methanol ($V_L = 1103 \text{ m s}^{-1}$)	118.32	73.69
Mercury ($V_L = 1450 \text{ m s}^{-1}$)	124.65	80.18
Coupling liquid	G (Gpa)	
	Dense	Porous
Water ($V_L = 1497 \text{ m s}^{-1}$)	58.73	37.43
Methanol ($V_L = 1103 \text{ m s}^{-1}$)	64.80	38.94
Mercury ($V_L = 1450 \text{ m s}^{-1}$)	60.09	43.84

Fig. 3a: V(z) acoustic signature of the system water/ Y123 $\text{YBa}_2\text{Cu}_3\text{O}_{7.8}$ at 30 MHzFig. 3b: V(z) acoustic signature of the system methanol/ Y123 $\text{YBa}_2\text{Cu}_3\text{O}_{7.8}$ at 30 MHzFig. 3c: V(z) acoustic signature of the system mercury/ Y123 $\text{YBa}_2\text{Cu}_3\text{O}_{7.8}$ at 30 MHz

periodic aspect in the dense case and is very fast (above 512 μm) for the porous material Fig. 3a. But in the case of methanol, both curves remain periodic with dense and porous material Fig. 3b. However, when Hg is used, the curves exhibit a perturbation in form of "flat pseudo-oscillations" and the attenuation is accentuated for the porous material Fig. 3c. There is a strong dependence of attenuation on Hg coupling due, probably, to Hg pressure penetration deficiency into pores and attributed to its surface strains.

The V(z) amplitude attenuation is a consequence of the surface microstructure state (pores and grain boundaries) and of the absorption of the coupling liquid which induces, generally, a difference between calculated and measured values. This is in good agreement with models which can be chosen to describe the dependence of attenuation on coupling and porosity^[12,15,16].

CONCLUSION

At lower temperatures the grain size is small and minimises microcracks where as at higher temperatures the grain started to growth and their size favours a relatively porous structure with micro cracks. During sintering, the appearance of liquid phase will inhibit the densification process leading to a "retrograde densification". The value 90% of theoretical density is not achieved, the material is still porous. It is difficult to predict the porosity distribution and its evolution because at sintering temperature there are several and different pore sizes.

Moreover, one has seen that both influence of coupling liquids and porosity are important on V_R , E and G parameters of the Y123 material. In both methanol and water, the V(z) curves are periodic and are adapted for

analysis and correspond well as coupling liquids. It seems that the choice of the coupling liquid and the frequency are fundamental for characterization. Several aspects suggest a role of coupling liquids and frequencies in attenuation in order to give comparable values of calculated and measured parameters.

The acoustic signature $V(z)$ determined for our synthesised Y123 material confirm its microstructure state through V_R , E and G values which are in good agreement with the studied experiments (dilatometry and porosimetry).

Our study will be extended to predictions giving for a given porosity an equivalent ultrasonic parameters V_R , E and G . Then, starting from the experimentally obtained V_L , V_R from $V(z)$ curves, we wish to establish the cartography of porosity fraction evolution (without damaging the samples by the immersion medium). This cartography can be enlarged to other acoustic parameters and allows, consequently, to give any porosity for any measured parameter.

REFERENCES

1. Mu, M.K. and J.R. Ashburn 1987. *And al. Phys. Rev. Lett.*, pp: 58-908.
2. Xu, 1998. *And al. Langmuir*, pp: 14.
3. Cathrine Housecroft and Alan Sharpe, 2005. *Inorganic Chemistry*. Second Edition. Pearson Education Limited. Essex, England.
4. Earnshaw and Greenwood, 2005. *Chmistry of the Elements*. Second Edition. Elsevier Butterworth-Heinemann. New York.
5. Lemons, R.A. and C.F. Quate, 1974. *Appl. Phys. Lett.*, 24: 163-165.
6. Briggs, A., 1992. Clarendon Press, Oxford.
7. Kushibiki, J. and N. Chubachi, 1967. *Electronics Lett.*, 10: 359-361.
8. Victorov, I.A., 1976. Plenum Press, New York.
9. Guerrioune, M., A. Boudour and Y. Boumaiza, 1998. *congres Euroméditerranéen*, Nantes.
10. Tsukahara, Y., C. Neron, C.K. Jen and J. Kushibiki, 1993. *Ultrasonic Symposium*, pp: 593-598.
11. Ledbetter, H., 1989. *Proc Japan Int. SAMPE, Symp.*, pp: 28-1.
12. Phani, K.K., S.K. Niyogi and J. Mater, 1987. *Sci.*, pp: 22-257.
13. Hasselman, D.P.H. and J.P. Sing, 1979. *Amer. Ceram. Bul.*, pp: 58-856.
14. Boudour, A., Y. Boumaiza, M. Guerrioune and S. Belkahla, 2004. *Physica status solidi (a)*, 201: 80-89.
15. Boumaiza, Y., R.J. Da Fonseca, J.M. Saurel, A. Foucaran, J.M. Camassel, E. Massone and T. Talierlio, 1995. *J. Mat. Sci.*, pp: 30 35-39.
16. Boumaiza, Y., Z. Hadjoub, A. Doghmane and L. Deboub, 1999. *J. Mat. Sci. Lett.*, pp: 18 295-297.